Journal Pre-proofs

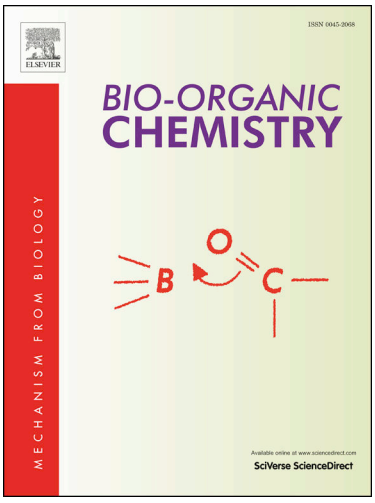

Extensive Investigation of Benzylic *N*-containing Substituents on the Pyrrolopyrimidine Skeleton as Akt Inhibitors with Potent Anticancer Activity

Yang Liu, Zhen Zhang, Fansheng Ran, Kaiwen Guo, Xin Chen, Guisen Zhao

PII: S0045-2068(19)32162-5
DOI: https://doi.org/10.1016/j.bioorg.2020.103671
Reference: YBIOO 103671

To appear in: *Bioorganic Chemistry*

Received Date: 18 December 2019
Revised Date: 7 February 2020
Accepted Date: 14 February 2020

Please cite this article as: Y. Liu, Z. Zhang, F. Ran, K. Guo, X. Chen, G. Zhao, Extensive Investigation of Benzylic *N*-containing Substituents on the Pyrrolopyrimidine Skeleton as Akt Inhibitors with Potent Anticancer Activity, *Bioorganic Chemistry* (2020), doi: https://doi.org/10.1016/j.bioorg.2020.103671

Extensive Investigation of Benzylic *N*-containing Substituents on the Pyrrolopyrimidine Skeleton as Akt Inhibitors with Potent Anticancer Activity

Yang Liu[1, 2], Zhen Zhang[1], Fansheng Ran[1], Kaiwen Guo[1], Xin Chen[1] and Guisen Zhao[1, *]

[1]*Department of Medicinal Chemistry, Key Laboratory of Chemical Biology (Ministry of Education), School of Pharmaceutical Sciences, Shandong University, Jinan, Shandong 250012, PR China;*

[2]*Department of Lymphoma & Myeloma, The University of Texas MD Anderson Cancer Center, Houston, TX 77030, USA.*

Corresponding author

Guisen Zhao*
Department of Medicinal Chemistry, School of Pharmaceutical Sciences, Shandong University, Jinan, Shandong 250012, PR China;
Tel/ Fax: +86 531 88382009;
E-mail: guisenzhao@sdu.edu.cn.

Abstract

Continuous optimization of benzylic substituents on 1-(4-(7*H*-pyrrolo[2,3-*d*]pyrimidin-4-yl)piperazin-1-yl)-2-phenylethan-1-one structure as Akt inhibitors was described in this paper. Particularly, compounds **8** and **14g** exhibited high enzymatic potency against all Akt isoforms and antiproliferative effects in mantle cell lymphoma cell lines, as well as favorable cytotoxicities in patient primary cancer cells. Low micromolar doses of both **8** and **14g** dose-dependently induced cell apoptosis and G_2/M cell cycle arrest, also suppressed the phosphorylation level of Akt downstream targets GSK3β and S6.

Keywords: Akt, Anticancer, Docking, Mantle cell lymphoma, Pyrrolopyrimidines

1. Introduction

PI3K/Akt signaling pathway is one of the most frequently activated pathways in human cancers, targeted agents against this pathway represent effective anticancer therapies [1]. Akt, a critical mediator in PI3K/Akt pathway, is an evolutionarily conserved serine/threonine kinase with three closely related isoforms, Akt1, Akt2 and Akt3, all of which share highly conserved domains: a N-terminal PH domain, a central kinase domain and a C-terminal regulatory domain [2]. Akt modulates cell survival and proliferation through pleiotropic downstream substrates such as glycogen synthase kinase 3 (GSK-3) and mammalian target of rapamycin complex 1 (mTORC1). Overexpression of Akt is a common feature identified in hematological neoplasms and solid tumors [3-5], and often associated with resistance to chemotherapy or radiotherapy [6]. Taken together, these factors would highly recommend Akt as a compelling target in cancer treatment [7].

Mantle cell lymphoma (MCL) is an uncommon subtype of B-cell non-Hodgkin lymphoma with rapid clinical evolution and unfavorable outcomes [8, 9]. Understanding the molecular pathophysiology for MCL has resulted in the identification of innovative targeted therapeutic agents [10]. Constitutive activation of Akt has been validated to contribution of pathogenesis and survival for mantle cell lymphoma [11], and considerable research efforts have validated that Akt inhibitors effectively decreased MCL tumor cell growth, suggesting Akt inhibition represents an innovative therapeutic strategy for MCL [12, 13].

Various attempts on structural optimization of pyrrolopyrimidine based ATP competitive inhibitors have been reported in our previous studies [14-16]. Inspired by the successful introduction of the rigid piperazine moiety, the benzylic position was taken as a continuous optimization site, with various

aliphatic amino groups and nitro-containing heterocycles introduced to explore further activity improvement on the pyrrolopyrimidine scaffold.

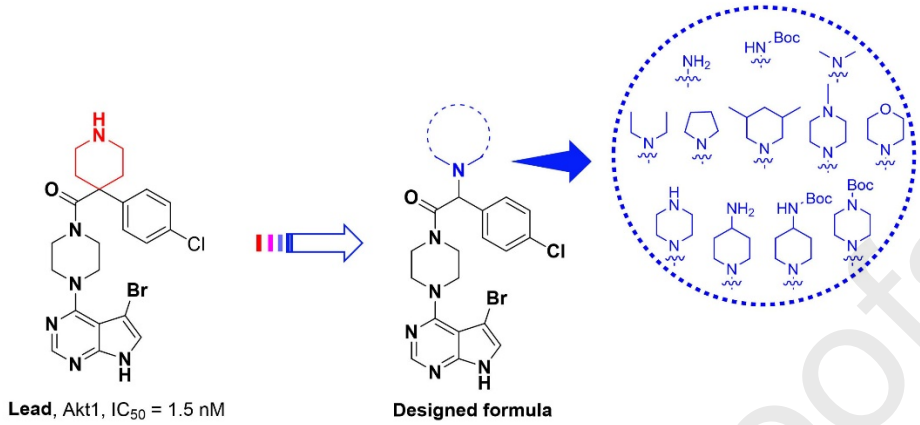

Fig. 1. Optimization schema for the designed compounds.

2. Results and discussion

2.1. Chemistry

The general synthetic route for the pyrrolopyrimidine derivatives is outlined in **Scheme 1**. Bromination on the 5-position of the commercially available **1** afforded compound **2**, subsequent introduction of the *tert*-butoxycarbonyl (Boc) protected piperazine linker via S_NAr delivered **3**, followed by removal of the Boc group affording **4** as dihydrochloride salts. Boc-protection of intermediate **5** and further amide coupling accomplished the first target compound **7**. Removal of the Boc moiety provided resultant **8** as hydrochloride salt.

Commercially available **9** reacted with methanol under H_2SO_4 condition to give **10**, followed by free radical reaction at the benzylic position produced **11**, which were further alkylated to give substituted amines **12a-12h**, subsequent ester hydrolysis gave the carboxylic acids **13a-13h**. Amide coupling between **13a-13h** and intermediate **4** yielded compounds **14a-14h**. Final deprotection of the Boc group accomplished target compounds **15a-15h**.

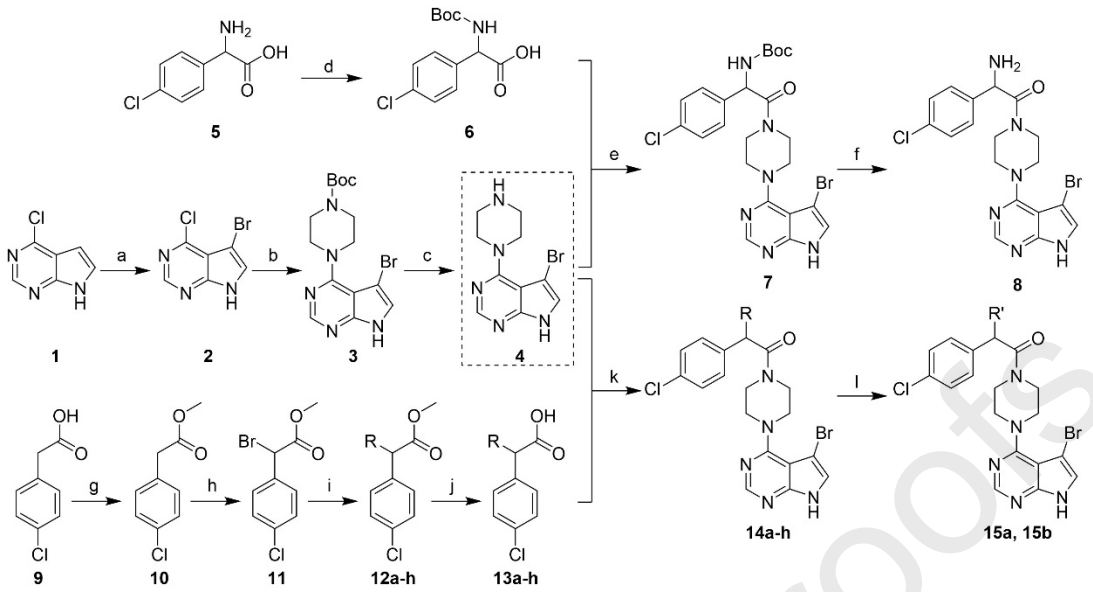

Scheme 1. Synthetic route for the designed derivatives. Reagents and conditions: (a) NBS, DMF, r.t.; (b) 1-Boc-piperazine, DIEA, DMF, 110°C; (c) HCl-dioxane, CH_3OH, r.t.; (d) $(Boc)_2O$, NaOH (aq), THF, r.t.; (e) EDCI, HOBt, DIEA, DMF, r.t.; (f) HCl-dioxane, CH_3OH, r.t.; (g) CH_3OH, H_2SO_4, 60°C; (h) NBS, AIBN, CCl_4, reflux; (i) Amines, DIEA, CH_3CN, 80°C; (j) CH_3CH_2OH, NaOH (aq, 10M), 80°C; (k) EDCI, HOBt, DIEA, DMF, r.t.; (l) HCl-dioxane, CH_3OH, r.t..

2.2. Akt inhibition and cell antiproliferative activity

The Akt1 inhibitory activities of the synthesized pyrrolopyrimidine compounds were determined via a Homogeneous Time-Resolved Fluorescence (HTRF) kinase activity assay. **GSK690693**, first Akt inhibitor entered clinical trials, was used as the positive control.

Table 1. The inhibitory effects of pyrrolopyrimidine derivatives on Akt1 activity

Code	R	Akt1 inhibition (%)		Code	R	Akt1 inhibition (%)	
		1 μM	50 nM			1 μM	50 nM
7		58.4	10.4	**14e**	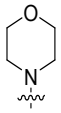	65.6	22.8
8		83.3	83.1	**14f**	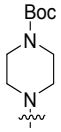	29.6	NA[a]
14a		88.5	73.0	**14g**	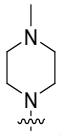	84.1	80.8
14b		81.8	78.0	**14h**	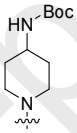	60.6	21.9
14c		95.5	52.6	**15a**	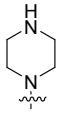	93.7	72.7
14d	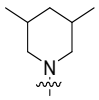	41.1	38.8	**15b**	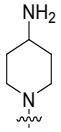	93.8	55.1
GSK690693		98.4	83.6				

[a]NA means not active

The structure-activity-relationship of the substituents at the benzylic position is shown in **Table 1**. The introduction of the free amino analogue **8** was proved to be the most potent resultant compound (83.1% inhibition at 50 nM), which showed comparable inhibitory activity to that of **GSK690693**. Dimethylamino and diethylamino substituents (**14a** and **14b**) decreased Akt1 inhibitory activities to a light degree, while most of the nitrogen-containing heterocyclic substitutions remarkably decreased the enzyme potency, except for methylpiperazine **14g** and piperazine **15a** (80.8% and 72.7% inhibition at 50 nM, respectively). The bulky Boc groups (**7, 14f** and **14h**) were not well tolerated at the benzylic position, which resulted in a substantial loss of enzyme potency.

Compounds with inhibition rate higher than 70% at 50 nM were further tested their antiproliferative effects against multiple MCL cell lines. **Ibrutinib**, a covalent BTK inhibitor approved

by FDA to treat MCL, was employed as positive control with **GSK690693**. In comparison with **GSK690693** and **ibrutinib**, all tested compounds displayed improved antiproliferative activities in MCL cell lines. As anticipated, compounds **8** and **14g** with preferable Akt1 enzyme potency also displayed favorable antiproliferative activities with IC_{50} values in low micromolar range.

Table 2. Cell proliferation assay assessing the effects of **8** and **14g** on MCL cell lines

Code	Cell viability assay, IC_{50} ± SD/μM[a]					
	Granta-519	**Mino**	**Jeko-1**	**Maver-1**	**Z-138**	**Rec-1**
Ibrutinib	10.5 ± 1.4	6.1 ± 1.4	2.5 ± 0.2	2.7 ± 1.2	2.8 ± 0.4	5.6 ± 0.4
GSK690693	18.5 ± 1.6	6.4 ± 0.2	3.3 ± 2.6	3.6 ± 2.1	5.1 ± 0.5	14.9 ± 1.7
8	1.3 ± 0.6	1.6 ± 0.1	1.3 ± 0.4	1.4 ± 0.2	1.1 ± 0.2	1.6 ± 0.6
14a	1.6 ± 0.5	1.6 ± 0.3	1.1 ± 0.1	1.9 ± 0.1	0.7 ± 0.2	0.9 ± 0.2
14b	2.6 ± 0.3	1.9 ± 0.8	1.9 ± 0.1	2.1 ± 0.3	1.6 ± 0.7	1.5 ± 0.4
14g	0.9 ± 0.3	1.1 ± 0.2	0.8 ± 0.1	0.7 ± 0.2	0.7 ± 0.1	0.6 ± 0.1
15a	2.5 ± 0.7	2.3 ± 0.4	1.4 ± 0.4	1.2 ± 0.6	1.4 ± 0.4	25.5 ± 2.7

[a]Values are means of three independent experiments

2.3 Akt isoforms selectivity assay

The FRET based Z'-LYTE kinase assay was used to determine the capability of compounds **8** and **14g** to inhibit all three Akt isoforms. The selectivity profile was summarized in **Table 3**, compounds **8** and **14g** were both validated as pan-Akt inhibitors with IC_{50} values in the low nanomolar range, and the IC_{50} values for Akt2 were within 3-7 folds of Akt1 and Akt3.

Table 3. Akt isoforms inhibitory profile of **8** and **14g**

Code	Akt kinase assay (IC_{50}, nM)		
	Akt1	**Akt2**	**Akt3**
8	3.2	20.9	6.2
14g	3.4	20.2	4.7

2.4. Cell apoptosis and cell cycle assay

To identify the mechanisms underlying the antiproliferative effects of these inhibitors, the efforts were focused on possible impact on cell apoptosis and cell cycle progression, which is mediated by Akt

downstream factors [17]. Accordingly, Annexin V/PI apoptosis and PI cell cycle assays were performed after **8** and **14g** treatment in Jeko-1 and Mino cells. **Fig. 2** and **Supplementary Fig. 1** show the dose dependent apoptosis after exposure of Jeko-1 and Mino cells to **8** or **14g** for 24 hours, suppression of the Akt downstream death promoter Bad was also validated by western blotting, as well as activated caspase-3 and cleaved PARP (**Fig. 3A**). Cell cycle assay demonstrated that **8** or **14g** treatment caused a significant G_2/M phase arrest in both Jeko-1 and Mino cells.

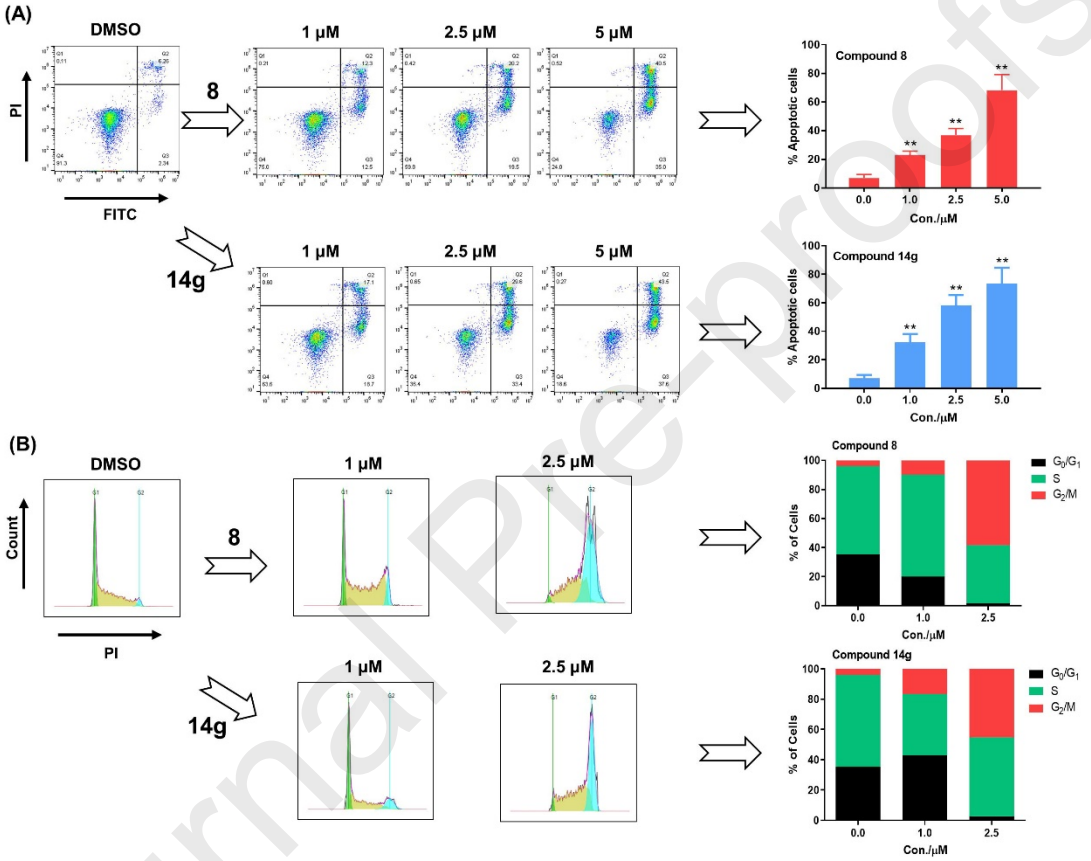

Fig. 2. Cell apoptosis (A) and cell cycle assay (B) in Jeko-1 cells after 24 hours treatment of **8** and **14g** at indicated concentrations. The data shown are the mean of three independent experiments. Statistical significance is indicated as *P < 0.05, **P < 0.01 compared to DMSO control.

2.5. Inhibitory effects on Akt signaling

Western blot analysis was performed to detect the capability of **8** and **14g** on the phosphorylation of Akt and its downstream effectors in Jeko-1 cells, in which PTEN loss has been validated as the genetic mutation that drives constitutively active PI3K/AKT signaling [18]. After 24 hours of treatment, both **8** and **14g** dose-dependently downregulated phosphorylated GSK3β and S6, which are major downstream targets of Akt (**Fig. 3A**). Hyperphosphorylation of the two Akt regulatory sites (Ser473 and Thr308) was also confirmed, which is consistent with the observations from certain

reported Akt inhibitors, proposing a possible positive feedback loop involved [19-21].

2.6. Cell viability assay in primary MCL cells

Cell viability assay was further performed for **8** and **14g** against the tumor cells isolated from two MCL patients (PT1 and PT2, **Supplemental Fig. 2**). As shown in **Fig. 3B**, **8** and **14g** dramatically decreased the cell viability of the two tested MCL patient cells compared to that of **GSK690693** and **ibrutinib**. Subsequent western blot validation on the primary cells was also in agreement with that observed in Jeko-1 cells (**Fig. 3C**).

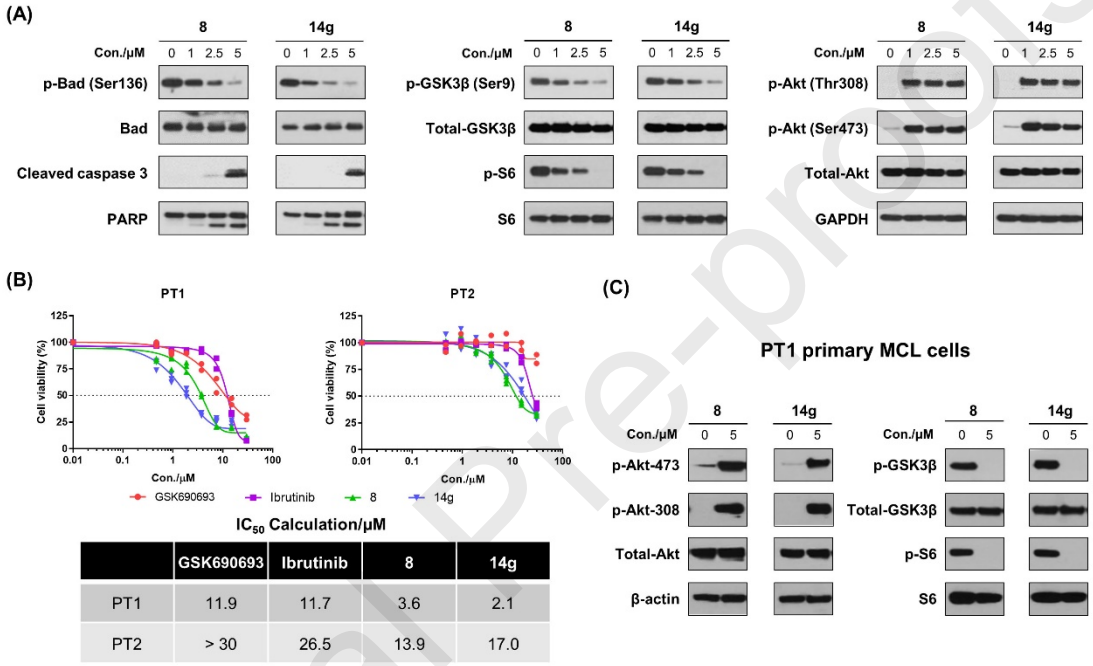

IC_{50} Calculation/μM

	GSK690693	Ibrutinib	8	14g
PT1	11.9	11.7	3.6	2.1
PT2	> 30	26.5	13.9	17.0

Fig. 3. Western blot analysis in Jeko-1 cells and efficacy validation in patient primary cancer cells. (A) Effects on apoptosis signaling and Akt signaling in Jeko-1 cells after 24 hours treatment of **8** and **14g**; (B) Cell viability assay in two primary MCL cells. Values were normalized to DMSO control; (C) Effect validation on Akt signaling of **8** and **14g** in PT1 primary cells.

2.7. Molecular modeling

The interaction modes between Akt1 and candidates **8** and **14g** were proposed and simulated by Sybyl 2.0, key interactions formed were highlighted and depicted in **Fig. 4**. Both inhibitors formed bidentate hydrogen bonds with residues Ala230 and Glu228 in the hinge region. The 4-chlorophenyl group projected into a hydrophobic pocket under the P-loop for hydrophobic contact. A beneficial hydrogen bond was formed between Glu234 and the primary amine of **8**, while the methylpiperazine moiety of **14g** interacted with residue Arg4 via two hydrogen bonds, which enhanced the favorable binding affinity for the resultant chimeric conformation.

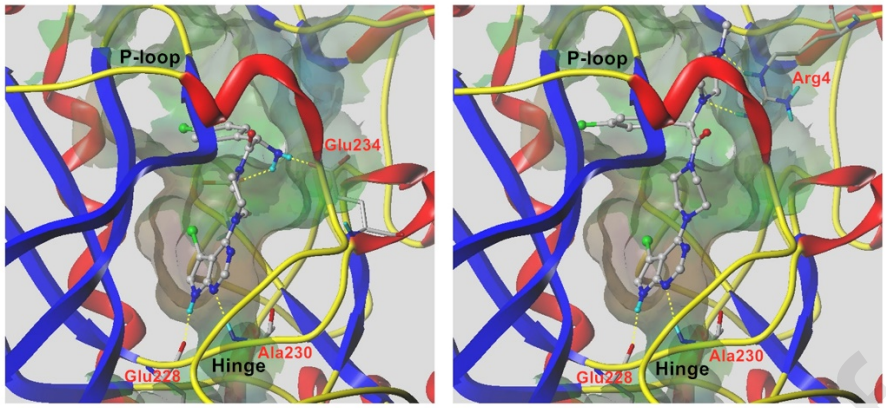

Fig. 4. Proposed binding modes of **8** (left) and **14g** (right) at the ATP binding site of Akt1 (PDB: 3MV5).

3. Conclusion

In summary, modification on the benzylic position of pyrrolopyrimidine core was extensively carried out. The promising pan-Akt inhibitors **8** and **14g** sustained the *in vitro* Akt1 inhibition and cellular inhibitory activity against multiple cancer cells, as well as desirable effects in patient primary cells, endorsing further development of the two candidates as anticancer agents.

4. Experimental section

4.1. Chemistry

All solvents and reagents were purchased from commercially available sources and used without further purification. Reactions were monitored by thin layer chromatography (TLC), and silica gel GF254 plates were used and visualized with UV light. Column chromatography was performed with silica gel using the solvents indicated. NMR spectra were recorded on a Bruker avance DRX600 or 400 Spectrometer using TMS as an internal standard in DMSO-d_6. Chemical shifts were reported in parts per million (ppm). Coupling constants (J) were given in Hz. The mass spectra (MS) were measured with an API 4000. All of the melting points were determined in a Büchi capillary melting point apparatus and are uncorrected. Human Akt1 was obtained from Carna Biosciences, Inc. (Canada). The HTRF assay kit was purchased from Cisbio assays, Inc. (France).

4.2. General synthesis of compounds

*4.2.1. General synthesis of compound **4***

The synthesis of **4** is the same as previously descried in our paper [14].

*4.2.2. Tert-butyl bis(2-chloroethyl)carbamate (**6**)*

To a solution of **5** (5 mmol) in tetrahydrofuran (20 mL), 10% sodium hydroxide solution (6 mmol)

was added. This was followed by addition of di-*tert*-butyl dicarbonate (7.5 mmol) over a period of 10 min at 0℃. Reaction mixture was stirred for 3 hours at room temperature after the addition, and acidified to pH 2 with 1N hydrochloric acid, the product thus obtained was extracted with ethyl acetate (3×50 mL). The organic layer was combined, washed with brine, dried over sodium sulfate and evaporated under reduced pressure to give the product **6** as a clear oil, yield 71.3%. Compound **6** was used directly for the next step without further purification.

4.2.3. General synthesis of compound 7

To a solution of **6** (1.75 mmol) and *N*, *N*-Diisopropylethylamine (DIEA, 8.75 mmol) in dimethylformamide (DMF, 2 mL) was added 1-(3-dimethylaminopropyl)-3-ethylcarbodiimide hydrochloride (EDCI) (2.1 mmol) and 1-hydroxybenzotriazole (HOBt) (2.1 mmoL). The reaction mixture was stirred at 0℃ for 1 hour, followed by addition of **4** (1.75 mmol). After completion of addition, the final mixture was stirred at room temperature for another 24 hours, then poured into ice water (20 mL), washed with saturated aqueous sodium bicarbonate (3×20 mL) and brine (3×20 mL), dried over sodium sulfate and solvent was evaporated under reduced pressure. The crude product was purified by silica gel chromatography eluting with dichloromethane /methanol (50:1) to give **7**. Brown solid, yield 43.8%, mp: 128~131℃, ^{1}H NMR (400 MHz, MeOD) δ (ppm): 8.24 (s, 1H), 7.39 (s, 4H), 7.34 (s, 1H), 5.67 (s, 1H), 3.95-3.84 (m, 1H), 3.84-3.72 (m, 2H), 3.72-3.64 (m, 1H), 3.64-3.53 (m, 2H), 3.53-3.42 (m, 1H), 3.31 (dt, *J* = 3.2, 1.6 Hz, 3H), 3.21-3.10 (m, 1H), 1.43 (s, 9H). ^{13}C NMR (100 MHz, MeOD) δ (ppm): 169.20, 159.69, 155.87, 151.33, 150.39, 136.03, 133.96, 129.35, 128.79, 123.95, 105.14, 86.58, 79.51, 54.66, 49.76, 49.50, 45.14, 42.12, 27.28. MS (ESI) m/z: 549 $[M+H]^{+}$.

*4.2.4. General synthesis of compounds **8***

7 (2 mmol) was suspended in methanol (2 mL), after addition of the 4M HCl in dioxane (3 ml), the reaction mixture was stirred for 48 hours at room temperature. The precipitate was filtrated, the obtained solid was recrystallized from methanol to give the desired **8**. Brown solid, yield: 72.5%, mp: 264~266℃, ^{1}H NMR (400 MHz, D_2O) δ (ppm): 8.08 (s, 1H), 7.39 (d, *J* = 8.6 Hz, 2H), 7.35 (d, *J* = 8.7 Hz, 2H), 7.32 (s, 1H), 5.50 (s, 1H), 3.99-3.88 (m, 1H), 3.86-3.73 (m, 1H), 3.71-3.47 (m, 5H), 3.46-3.34 (m, 1H), 3.02-2.90 (m, 1H). ^{13}C NMR (100 MHz, D_2O) δ (ppm): 166.38, 154.28, 146.67, 143.18, 136.26, 130.14, 129.94, 129.51, 126.60, 103.01, 88.85, 66.52, 54.53, 49.63, 48.75, 44.33, 41.97. MS (ESI) m/z: 449 $[M+H]^{+}$.

*4.2.5. General synthesis of compounds **10***

A solution of **9** (40 mmol) in dry methanol (25 mL) was treated with 5 drops of concentrated H_2SO_4 (cat.) at room temperature. The reaction resulting mixture was stirred and heated at reflux for 5 hours to completion and was concentrated under reduced pressure. The crude product was dissolved in 25 mL ethyl acetate, washed with saturated aqueous sodium bicarbonate, water (3×25mL) and brine (3×25mL), dried over Na_2SO4, filtered and concentrated to get the titled compound 10 as a yellow oil, yield 97.6%, ^{1}H NMR (400 MHz, DMSO-d_6) δ (ppm): 7.39 (d, J = 8.4 Hz, 2H), 7.30 (d, J = 8.4 Hz, 2H), 3.70 (d, 2H), 3.61 (s, 3H). MS (ESI) m/z: 185 $[M+H]^+$.

*4.2.6. General synthesis of compounds **11***

To a solution of ethyl 4-pyridylacetate (27.95 mmol) in carbon tetrachloride (20 mL), N-bromosuccinimide (27.95 mmol) and Azobisisobutyronitrile (AIBN, 7.95 mmol) were added. The reaction mixture was heated at reflux for 2 hours after which the solids were removed by filtration. The organics filtrate was concentrated under reduced pressure. The resulting crude oil was purified by flash chromatography on silica gel to obtain as a yellow oil, 94.3%, ^{1}H NMR (400 MHz, DMSO-d_6) δ (ppm): 7.59 (d, J = 8.4 Hz, 2H), 7.49 (d, J = 8.4 Hz, 2H), 6.00 (s, 1H), 3.73 (s, 3H). MS (ESI) m/z: 263 $[M+H]^+$.

*4.2.7. General synthesis of compounds **12***

To a solution of compound **11** (2 mmol) in acetonitrile (5 mL) was added substituted amine (2.2 mmol) and DIEA (3 mmol) at room temperature. The reaction mixture was refluxed for 4 hours and then the solvent was evaporated in vacuo. The resultant residue was diluted with ethyl acetate (20 mL), washed with water and brine (3×20 mL), dried over Na_2SO_4.The mixture was then filtered and the filtrate was concentrated in vacuo. The resulting residue was purified by flash column chromatography with ether/ethylacetate (1/3) to afford **12**.

*4.2.7.1. Methyl 2-(4-chlorophenyl)-2-(dimethylamino)acetate (**12a**)*

Yellow oil, yield 61.8%, ^{1}H NMR (400 MHz, $CDCl_3$) δ (ppm): 7.39 (d, J = 8.8 Hz, 2H), 7.33 (d, J = 8.8 Hz, 2H), 3.86 (s, 1H), 3.70 (s, 3H), 2.24 (s, 6H). MS (ESI) m/z: 228 $[M+H]^+$.

*4.2.7.2. Methyl 2-(4-chlorophenyl)-2-(diethylamino)acetate (**12b**)*

Yellow oil, yield 70.2%, ^{1}H NMR (400 MHz, $CDCl_3$) δ (ppm): 7.39 (d, J = 8.4 Hz, 2H), 7.31 (d, J = 8.8 Hz, 2H), 3.94 (s, 1H), 3.68 (s, 3H), 2.36 (q, 4H), 1.60 (t, 6H). MS (ESI) m/z: 256 $[M+H]^+$.

*4.2.7.3. Methyl 2-(4-chlorophenyl)-2-(pyrrolidin-1-yl)acetate (**12c**)*

Colorless oil, yield 90%, ^{1}H NMR (400 MHz, $CDCl_3$) δ (ppm): 7.43 (d, J = 8.4 Hz, 2H), 7.32 (d, J = 8.4 Hz, 2H), 3.90 (s, 1H), 3.68 (s, 3H), 2.55-2.43 (m, 4H), 1.82-1.81 (m, 4H). MS (ESI) m/z: 254

$[M+H]^+$.

*4.2.7.4. Methyl 2-(4-chlorophenyl)-2-(3,5-dimethylpiperidin-1-yl)acetate (**12d**)*

Colorless oil, yield 65.7%, ^{1}H NMR (400 MHz, $CDCl_3$) δ (ppm): 7.31-7.26 (m, 4H), 4.45 (s, 1H), 3.69 (s, 3H), 2.73-2.67 (m, 2H), 2.70-1.84 (m, 6H), 1.07 (t, J = 6.0 Hz, 6H). MS (ESI) m/z: 296 $[M+H]^+$.

*4.2.7.5. Methyl 2-(4-chlorophenyl)-2-morpholinoacetate (**12e**)*

Clear oil, yield 71.4%, ^{1}H NMR (400 MHz, DMSO-d_6) δ (ppm): 7.45 (d, J = 9.2 Hz, 2H), 7.43 (d, J = 9.2 Hz, 2H), 4.16 (s, 1H), 3.61 (s, 3H), 3.57 (d, J = 4.4 Hz, 4H), 2.35 (d, J = 4.4 Hz, 4H). MS (ESI) m/z: 270 $[M+H]^+$.

*4.2.7.6. Tert-butyl 4-(1-(4-chlorophenyl)-2-methoxy-2-oxoethyl)piperazine-1-carboxylate (**12f**)*

Clear oil, yield 99.5%, ^{1}H NMR (400 MHz, $CDCl_3$) δ (ppm): 7.38 (d, J = 8.4 Hz, 2H), 7.33 (d, J = 8.4 Hz, 2H), 3.99 (s, 1H), 3.69 (s, 3H), 3.44 (s, 4H), 2.39 (s, 4H), 1.44 (s, 9H). MS (ESI) m/z: 369 $[M+H]^+$.

*4.2.7.7. Methyl 2-(4-chlorophenyl)-2-(4-methylpiperazin-1-yl)acetate (**12g**)*

Brown oil, yield 66.7%, ^{1}H NMR (400 MHz, $CDCl_3$) δ (ppm): 7.39 (d, J = 8.4 Hz, 2H), 7.32 (d, J = 8.4 Hz, 2H), 3.96 (s, 1H), 3.68 (s, 3H), 2.63-2.40 (m, 8H), 2.31 (s, 3H). MS (ESI) m/z: 283 $[M+H]^+$.

*4.2.7.8. Methyl 2-(4-((tert-butoxycarbonyl)amino)piperidin-1-yl)-2-(4-chlorophenyl)acetate (**12h**)*

White solid, yield 70.6%, ^{1}H NMR (400 MHz, $CDCl_3$) δ (ppm): 7.37 (d, J = 8.4 Hz, 2H), 7.32 (d, J = 8.4 Hz, 2H), 4.43 (br, 1H), 3.96 (s, 1H), 3.68 (s, 3H), 3.49 (br, 1H), 2.86 (br, 1H), 2.67 (br, 1H), 2.24 (t, J = 10.8 Hz, 1H), 2.01-1.84 (m, 3H), 1.45-1.43 (s, 10H). MS (ESI) m/z: 383 $[M+H]^+$.

*4.2.8. General synthesis of compounds **13***

To a solution of 12 (1 mmol) in 3 mL of ethanol/water (2/1), 2mL of 1 N aqueous sodium hydroxide solution (2 mmol) were added and the mixture was stirred at room temperature for 4 hours. The organic solvents were removed under reduced pressure and the resulting aqueous solution was adjusted in an ice bath to pH 6 using 1 N aqueous hydrochloric acid. The resulting solid was filtered, washed with water to obtain 13.

*4.2.8.1. 2-(4-Chlorophenyl)-2-(dimethylamino)acetic acid (**13a**)*

White solid, yield 81.5%, ^{1}H NMR (400 MHz, $CDCl_3$) δ (ppm): 7.41 (d, J = 7.2 Hz, 2H), 7.16 (d, J = 7.2 Hz, 2H), 4.77 (s, 1H), 2.84 (s, 6H). MS (ESI) m/z: 212 $[M-H]^-$.

*4.2.8.2. 2-(4-Chlorophenyl)-2-(diethylamino)acetic acid (**13b**)*

White solid, yield 20%, ^{1}H NMR (400 MHz, MeOD) δ (ppm): 7.64-7.54 (m, 2H), 7.48-7.41 (m, 2H), 4.56 (s, 1H), 3.21 (td, J = 13.3, 6.4 Hz, 2H), 3.05 (s, 2H), 1.25 (t, J = 7.1 Hz, 6H). MS (ESI) m/z:

240 [M-H]$^-$.

*4.2.8.3. 2-(4-Chlorophenyl)-2-(pyrrolidin-1-yl)acetic acid (**13c**)*

White solid, yield 86.9%, ^{1}H NMR (400 MHz, CD_3OD) δ (ppm): 7.56 (d, J = 8.8 Hz, 2H), 7.46 (d, J = 8.4 Hz, 2H), 4.51 (s, 1H), 3.31-3.29 (m, 4H), 2.11-1.99 (m, 4H). MS (ESI) m/z: 238 [M-H]$^-$.

*4.2.8.4. 2-(4-Chlorophenyl)-2-(3,5-dimethylpiperidin-1-yl)acetic acid (**13d**)*

White solid, yield 58.8%, ^{1}H NMR (400 MHz, DMSO-d_6) δ (ppm): 7.43 (d, J = 8.8 Hz, 2H), 7.35 (d, J = 8.8 Hz, 2H), 3.81 (s, 1H), 3.09-3.07 (m, 1H), 2.56-2.54 (m, 1H), 1.70-1.63 (m, 4H), 1.51 (t, J = 10.8 Hz, 1H), 0.80 (d, J = 5.2 Hz, 3H), 0.70 (d, J = 8.4 Hz, 3H), 0.54-0.45 (m, 1H). MS (ESI) m/z: 280 [M-H]$^-$.

*4.2.8.5. 2-(4-Chlorophenyl)-2-morpholinoacetic acid (**13e**)*

White solid, yield 83.9%, ^{1}H NMR (400 MHz, CD_3OD) δ (ppm): 7.55 (d, J = 8.4 Hz, 2H), 7.45 (d, J = 8.8 Hz, 2H), 4.41 (s, 1H), 3.88-3.81 (m, 3H), 3.30-3.22 (m, 3H), 2.88-2.85 (m, 2H). MS (ESI) m/z: 254 [M-H]$^-$.

*4.2.8.6. 2-(4-(Tert-butoxycarbonyl)piperazin-1-yl)-2-(4-chlorophenyl)acetic acid (**13f**)*

White solid, yield 43.4%, ^{1}H NMR (400 MHz, DMSO-d_6) δ (ppm): 7.45 (d, J = 8.8 Hz, 2H), 7.42 (d, J = 8.8 Hz, 2H), 4.05 (s, 1H), 3.30-3.24 (m, 4H), 2.37-2.29 (m, 4H), 1.37 (s, 9H). MS (ESI) m/z: 353 [M-H]$^-$.

*4.2.8.7. Methyl 2-(4-chlorophenyl)-2-(4-methylpiperazin-1-yl)acetate (**13g**)*

Paleyellow solid, yield 93.9%, ^{1}H NMR (400 MHz, CD_3OD-d_6) δ (ppm): 7.50 (d, J = 8.4 Hz, 2H), 7.34 (d, J = 8.4 Hz, 2H), 3.88 (s, 1H), 3.31-3.30 (m, 3H), 3.14 (s, 3H), 2.74 (s, 3H), 2.65 (br, 2H). MS (ESI) m/z: 267 [M-H]$^-$.

*4.2.8.8. 2-(4-((Tert-butoxycarbonyl)amino)piperidin-1-yl)-2-(4-chlorophenyl)acetic acid (**13h**)*

White solid, yield 59.8%, ^{1}H NMR (400 MHz, DMSO-d_6) δ (ppm): 7.42 (s, 4H), 6.84 (d, J = 7.2 Hz, 1H), 4.04 (s, 1H), 3.26 (s, 1H), 3.05 (d, J = 11.2 Hz, 1H), 2.64 (d, J = 11.6 Hz, 1H), 2.36 (t, J = 10.8 Hz, 1H), 2.23 (t, J = 10.8 Hz, 1H), 1.75 (d, J = 6.0 Hz, 1H), 1.68 (d, J = 12.4 Hz, 1H), 1.50 (t, J = 12.0 Hz, 2H), 1.36 (s, 9H). MS (ESI) m/z: 367 [M-H]$^-$.

*4.2.9. General synthesis of compounds **14***

To a solution of **13a-13h** (0.4 mmol) and DIEA (2.0 mmol) in DMF (2 mL) was added EDCI (0.48 mmol) and HOBt (0.48 mmoL). The reaction mixture was stirred at 0℃ for 1 hour, followed by addition of **4** (0.40 mmol). After completion of addition, the final mixture was stirred at room temperature for

another 12 hours, then poured into ice water (20 mL), extractd with ethyl acetate (20×2 mL), the combined organic layer was washed with saturated aqueous sodium bicarbonate (20×3 mL) and brine (20×2 mL), dried over sodium sulfate and solvent was evaporated under reduced pressure. The crude product was purified by silica gel chromatography eluting with ethyl acetate /methanol (100:1~60:1) to give **14**.

*4.2.9.1. 1-(4-(5-Bromo-7H-pyrrolo[2,3-d]pyrimidin-4-yl)piperazin-1-yl)-2-(4-chlorophenyl)-2-(dimethylamino)ethan-1-one (**14a**)*

Brown solid, yield 74.4%, mp: 103~105℃, ^{1}H NMR (400 MHz, $CDCl_3$) δ (ppm): 12.06 (s, 1H), 8.37 (s, 1H), 7.40 (d, *J* = 8.5 Hz, 2H), 7.34 (d, *J* = 8.5 Hz, 2H), 7.29 (s, 1H), 4.26 (s, 1H), 3.95-3.91 (m, 1H), 3.88-3.62 (m, 4H), 3.59-3.50 (m, 2H), 3.33-3.19 (m, 1H), 2.32 (s, 6H), 1.26 (t, *J* = 7.1 Hz, 1H). ^{13}C NMR (100 MHz, $CDCl_3$) δ (ppm): 169.27, 159.67, 151.95, 150.63, 134.55, 134.21, 130.33, 129.00, 123.49, 105.36, 87.34, 71.55, 50.38, 49.59, 45.29, 43.39, 42.12. MS (ESI) m/z: 477 $[M+H]^+$.

*4.2.9.2. 1-(4-(5-Bromo-7H-pyrrolo[2,3-d]pyrimidin-4-yl)piperazin-1-yl)-2-(4-chlorophenyl)-2-(diethylamino)ethan-1-one (**14b**)*

Brown solid, yield 62.3%, mp: 83~87℃, ^{1}H NMR (400 MHz, $CDCl_3$) δ (ppm): 11.78 (s, 1H), 8.41 (s, 1H), 7.39 (d, *J* = 8.3 Hz, 2H), 7.34 (d, *J* = 8.4 Hz, 2H), 4.84 (s, 1H), 3.94-3.81 (m, 3H), 3.71-3.55 (m, 4H), 3.49-3.40 (m, 1H), 2.81 (dd, *J* = 13.2, 6.8 Hz, 2H), 2.63 (dd, *J* = 13.1, 6.7 Hz, 2H), 1.28 (s, 2H), 1.03 (t, *J* = 7.0 Hz, 6H). ^{13}C NMR (100 MHz, $CDCl_3$) δ (ppm): 170.11, 159.73, 151.91, 150.50, 135.28, 133.74, 130.66, 128.68 (2C), 123.50 (2C), 105.38, 87.34, 65.77, 50.45, 49.75, 45.30, 44.33 (2C), 41.90, 29.71, 13.04 (2C). MS (ESI) m/z: 505 $[M+H]^+$.

*4.2.9.3. 1-(4-(5-Bromo-7H-pyrrolo[2,3-d]pyrimidin-4-yl)piperazin-1-yl)-2-(4-chlorophenyl)-2-(pyrrolidin-1-yl)ethan-1-one (**14c**)*

Brown solid, yield 64.6%, mp: 112~115℃, ^{1}H NMR (400 MHz, $CDCl_3$) δ (ppm): 11.87 (s, 1H), 8.36 (s, 1H), 7.38 (dd, *J* = 42.1, 7.4 Hz, 4H), 4.37 (s, 1H), 3.71 (dd, *J* = 98.1, 45.4 Hz, 7H), 3.26 (s, 1H), 2.61 (d, *J* = 26.6 Hz, 4H), 1.81 (s, 4H). ^{13}C NMR (100 MHz, DMSO) δ (ppm): 168.76, 159.55, 152.09, 151.09, 132.91, 130.84, 128.90 (2C), 124.84 (2C), 104.96, 86.24, 67.78, 51.74, 50.30 (2C), 45.24 (2C), 42.02 (2C), 23.44 (2C), 14.55. MS (ESI) m/z: 503 $[M+H]^+$.

*4.2.9.4. 1-(4-(5-Bromo-7H-pyrrolo[2,3-d]pyrimidin-4-yl)piperazin-1-yl)-2-(4-chlorophenyl)-2-(3,5-dimethylpiperidin-1-yl)ethan-1-one (**14d**)*

Brown solid, yield 51.0%, mp: 114~117℃, ^{1}H NMR (400 MHz, $CDCl_3$) δ (ppm): 11.85 (s, 1H),

8.38 (s, 1H), 7.38 (d, *J* = 8.5 Hz, 2H), 7.33 (d, *J* = 8.5 Hz, 2H), 4.39 (s, 1H), 3.95-3.71 (m, 4H), 3.70-3.47 (m, 3H), 3.47-3.33 (m, 1H), 2.85 (t, *J* = 8.3 Hz, 2H), 1.83-1.62 (m, 4H), 1.54-1.43 (m, 1H), 1.25 (s, 2H), 0.83-0.78 (m, 6H), 0.55-0.47 (m, 1H). ^{13}C NMR (100 MHz, $CDCl_3$) δ (ppm): 169.38, 159.70, 151.92, 150.65, 133.82, 130.54, 128.72, 123.23, 105.30, 87.52, 71.53, 59.43, 58.51, 50.39, 49.70, 45.26, 42.10, 31.94, 31.34, 31.15, 29.71, 29.38, 22.71, 19.61, 14.15. MS (ESI) m/z: 545 $[M+H]^+$.

*4.2.9.5. 1-(4-(5-Bromo-7H-pyrrolo[2,3-d]pyrimidin-4-yl)piperazin-1-yl)-2-(4-chlorophenyl)-2-morpholinoethan-1-one (**14e**)*

Brown solid, yield 70.0%, mp: 110~114℃, ^{1}H NMR (400 MHz, $CDCl_3$) δ (ppm): 11.91 (s, 1H), 8.38 (s, 1H), 7.40 (d, *J* = 8.5 Hz, 2H), 7.35 (d, *J* = 8.5 Hz, 2H), 7.28 (s, 1H), 4.00-3.62 (m, 10H), 3.56 (dd, *J* = 16.1, 11.5 Hz, 2H), 3.30 (dd, *J* = 10.0, 7.3 Hz, 1H), 2.55 (s, 4H). ^{13}C NMR (100 MHz, $CDCl_3$) δ (ppm): 168.65, 159.67, 151.92, 150.64, 134.38, 133.47, 130.45, 129.06, 123.33, 105.36, 87.45, 71.15, 66.89, 60.43, 51.75, 50.38, 49.58, 45.30, 42.15. MS (ESI) m/z: 519 $[M+H]^+$.

*4.2.9.6. Tert-butyl 4-(2-(4-(5-bromo-7H-pyrrolo[2,3-d]pyrimidin-4-yl)piperazin-1-yl)-1-(4-chlorophenyl)-2-oxoethyl)piperazine-1-carboxylate (**14f**)*

Brown solid, yield 76.2%, mp: 131~135℃, ^{1}H NMR (400 MHz, $CDCl_3$) δ (ppm): 12.02 (s, 1H), 8.30 (s, 1H), 7.40-7.23 (m, 4H), 7.20 (s, 1H), 4.30 (s, 1H), 3.93-3.14 (m, 12H), 2.58-2.28 (m, 4H), 1.36 (s, 10H). MS (ESI) m/z: 618 $[M+H]^+$.

*4.2.9.7. 1-(4-(5-Bromo-7H-pyrrolo[2,3-d]pyrimidin-4-yl)piperazin-1-yl)-2-(4-chlorophenyl)-2-(4-methylpiperazin-1-yl)ethan-1-one (**14g**)*

Brown solid, yield 51.6%, mp: 85~87℃, ^{1}H NMR (400 MHz, $CDCl_3$) δ (ppm): 8.37 (s, 1H), 7.39 (d, *J* = 8.5 Hz, 2H), 7.33 (d, *J* = 8.5 Hz, 2H), 7.26 (s, 1H), 4.31 (s, 1H), 3.95-3.46 (m, 8H), 3.32 (dd, *J* = 10.0, 7.2 Hz, 1H), 2.54 (d, *J* = 26.6 Hz, 7H), 2.28 (s, 3H). ^{13}C NMR (100 MHz, $CDCl_3$) δ (ppm): 168.87, 159.67, 151.96, 150.68, 134.12, 133.92, 130.37, 128.91, 123.42, 105.37, 87.31, 71.28, 54.95, 51.17, 50.38, 49.63, 46.08, 45.87, 45.26, 42.19, 10.76. MS (ESI) m/z: 532 $[M+H]^+$.

*4.2.9.8. Tert-butyl (1-(2-(4-(5-bromo-7H-pyrrolo[2,3-d]pyrimidin-4-yl)piperazin-1-yl)-1-(4-chlorophenyl)-2-oxoethyl)piperidin-4-yl)carbamate (**14h**)*

Brown solid, yield 54.5%, mp: 140~143℃, ^{1}H NMR (400 MHz, $CDCl_3$) δ (ppm): 11.63 (s, 1H), 8.36 (s, 1H), 7.37 (d, *J* = 8.5 Hz, 2H), 7.33 (d, *J* = 8.5 Hz, 2H), 4.42 (d, *J* = 52.5 Hz, 2H), 3.93-3.40 (m, 9H), 3.32 (s, 1H), 3.00-2.75 (m, 2H), 2.32 (s, 1H), 2.19-1.99 (m, 2H), 1.91 (t, *J* = 14.5 Hz, 2H), 1.58-1.35 (m, 12H). MS (ESI) m/z: 632 $[M+H]^+$.

*4.2.10. General synthesis of compounds **15a-15b***

Compounds **14a-14b** (0.1 mmol) was suspended in methanol (2 mL), after addition of the 4M HCl in dioxane (6 ml), the reaction mixture was stirred for 48 hours at room temperature. The precipitate was filtrated, the obtained solid was recrystallized from methanol to give the desired **15a-15b**.

*4.2.10.1. 1-(4-(5-Bromo-7H-pyrrolo[2,3-d]pyrimidin-4-yl)piperazin-1-yl)-2-(4-chlorophenyl)-2-(piperazin-1-yl)ethan-1-one hydrochloride (**15a**)*

White solid, yield 98.9%, mp: 150~155℃, ^{1}H NMR (400 MHz, D_2O) δ (ppm): 8.10 (s, 1H), 7.43 (s, 5H), 7.35 (s, 1H), 5.54 (s, 1H), 4.05-3.94 (m, 1H), 3.83 (qd, *J* = 12.9, 4.5 Hz, 2H), 3.76-3.68 (m, 1H), 3.67-3.30 (m, 15H), 3.29-3.16 (m, 3H), 2.93-2.82 (m, 1H). ^{13}C NMR (100 MHz, D_2O) δ (ppm): 164.96, 154.30, 146.52, 143.05, 137.33, 131.14, 130.53, 126.65, 125.98, 103.02, 88.91, 69.29, 49.61, 48.51, 48.08, 44.45, 42.06, 40.80. MS (ESI) m/z: 518 $[M+H]^+$.

*4.2.10.2. 2-(4-Aminopiperidin-1-yl)-1-(4-(5-bromo-7H-pyrrolo[2,3-d]pyrimidin-4-yl)piperazin-1-yl)-2-(4-chlorophenyl)ethan-1-one hydrochloride (**15b**)*

White solid, yield 99.2%, mp: 147~151℃, ^{1}H NMR (400 MHz, D_2O) δ (ppm): 8.11 (s, 1H), 7.45 (s, 5H), 7.37 (s, 1H), 5.52 (s, 1H), 4.09-3.96 (m, 1H), 3.97-3.28 (m, 14H), 3.26-2.81 (m, 6H), 2.27-2.21 (m, 3H), 2.05-1.76 (m, 3H). ^{13}C NMR (100 MHz, D_2O) δ (ppm): 164.76, 154.54, 151.00, 146.71, 143.36, 137.35, 130.49, 130.42, 126.57, 125.95, 103.14, 88.81, 66.52, 62.47, 49.57, 49.02, 48.49, 45.23, 44.46, 44.28, 42.10. MS (ESI) m/z: 532 $[M+H]^+$.

4.3. In vitro Akt1 kinase activity assay

The *in vitro* Akt1 kinase activity was evaluated via an HTRF assay (LANCE®) using the Akt kinase kit (Cisbio Bioassays, No.62ST3PEB) in 384-well plates. Each well was added Akt1, STK Substrate-biotin, tested compounds and ATP in kinase buffer (50 mM HEPES, 5 mM $MgCl_2$, 1 mM DTT, 0.02% NaN_3 and 0.01% BSA, pH = 7.0) in sequence, then incubated for 45 min at 25°C. Finally, Sa-XL665 and STK Ab-Cryptate were added to stop the enzymatic step and incubated for 2 hours to finish the detection process. The ratio (665 nm/620 nm) was obtained using a microplate reader (Perkin Elmer, USA).

4.4 Z'-LYTE Kinase Assay

The reaction was conducted in a 384-well plate with 10 μL reaction volume per well containing 2 μM Ser/Thr 06 peptide substrate in 50 mM HEPES pH 7.5, 0.01% BRIJ-35, 10 mM MgCl2, 1 mM EGTA and appropriate amount of AKT kinases with a serial 3-fold dilution of tested compound. The final

reaction concentration of ATP was 75 μM for Akt1, 200 μM for Akt2 and 100 μM for Akt3. After 1 hour kinase reaction incubation, 5 μL of a 1:4096 dilution of development reagent A is added, reaction was developed for another 1 hour and then terminated. Fluorescein FRET signal were monitored at 445 and 520 nm, respectively. The fluorescence ratio was calculated according to the manufacturer's protocol (ThermoFisher, USA).

4.5. Cell lines and primary MCL cells

MCL cell lines Granta519, Maver-1, Rec-1, Z-138, Mino and Jeko-1 were purchased from the American Type Culture Collection (ATCC). Human MCL cells were purified from the apheresis of MCL patients after obtaining informed consent and approval by the Institutional Review Board at The University of Texas MD Anderson Cancer Center. Patient peripheral blood mononuclear cells (PBMCs) were isolated by Ficoll-Hypaque density centrifugation and stained for human anti-CD5 and human anti-CD20 antibodies, CD5 and CD20 double positive cells representing MCL cell population were detected by Novocyte Flow Cytometer (ACEA Bioscience, USA). Isolated samples with more than 95% $CD5^+CD20^+$ MCL cells were used without further purification. Cells were further cultured in RPMI-1640, supplemented with 10% heat-inactivated fetal bovine serum, 2% HEPES buffer and penicillin (10,000 units/mL; Sigma), streptomycin (10 mg/mL; Sigma).

4.6. Cell proliferation assay

Cell proliferation assay was performed on a panel of MCL cell lines and primary MCL cells using the CellTiter-Glo Luminescent cell viability assay kit (Promega) following the manufacturer's protocol. In short, cells were plated in 96-well plates at a density of 1×10^4 cells/well for cell lines and 12.5×10^4 cells/well for primary MCL cells, then treated with DMSO and different concentrations of the synthesized compounds and incubated in a humidified atmosphere with 5% CO_2 at 37°C for 72 hours on MCL cell lines and 24 hours on primary MCL cells. IC_{50} values were calculated using the Graphpad prism 6 software.

4.7. Cell apoptosis assay

Apoptosis was quantified by Annexin V/Propidium Iodide (PI)-binding assay. Cells were seeded in 6-well plates with 1 μM, 2.5 μM and 5 μM of **8** and **14g** for 24 hours. Treated cells were washed twice with cold phosphate-buffered saline (PBS) and then resuspended in100 μL binding buffer, to which 2 μL of Annexin V-FITC and 5 μL of PI were added. The samples were gently vortexed and incubated for 15 minutes at room temperature in the dark. After addition of 200 μL binding buffer, samples were

immediately analyzed by flow cytometry using a NovoCyte Flow Cytometer (ACEA Biosciences, San Diego, CA). The number of apoptotic cells was determined using the NovoExpress software.

4.8. Cell cycle assay

Cell cycle arrest was measured using PI staining by flow cytometry. Cells was seeded in 6-well plates with 1 μM and 2.5 μM of **8** and **14g** for 24 hours, then cells were harvested, washed twice with cold PBS, and subsequent fixing in cold 70% ethanol overnight at 4 ℃. Then samples were washed twice with PBS, followed by further treatment with 50 uL of 100 ug/mL ribonuclease and 200 uL 50 ug/mL PI, and finally analyzed by NovoCyte Flow Cytometer (ACEA Biosciences, San Diego, CA).

4.9. Western blotting

Jeko-1 cells and patient primary cells were cultured with different concentrations of **8** and **14g** for 24 hours. Then cells were harvested and lysed in a lysis buffer (Cell Signaling, Danvers, MA). The cell lysates were kept on ice for 30 minutes and centrifuged at 12,000×rpm for 20 minutes at 4^{o}C. The protein concentration was determined by the Bradford assay (Bio-Rad, Hercules, CA). Twenty micrograms of sample proteins were mixed with the loading buffer and separated by 10% SDS-PAGE. The proteins were then transferred onto methanol equilibrated PVDF membrane (BIO-RAD Laboratories, 162-0177), which was blocked for 1 hour in 5% nonfat dry milk in TBST (BD Bioscience, San Jose, CA). The membranes were incubated with a primary antibody overnight at 4 ℃. Secondary antibodies were added for 1 hour at room temperature. Finally, the membrane was visualized by ECL (Perkin Elmer Life Sciences, NE104001EA). Antibodies against PARP, cleaved caspase 3, p-Akt-308, p-Akt-473, pan-Akt, p-GSK3β, total- GSK3β and GAPDH were obtained from Cell Signaling.

4.10. Molecular docking

Molecular docking was performed using the Sybyl 2.0 software package and the Akt1 crystal structure (PDB: 3MV5) was retrieved from the Protein Data Bank. Protein preparation was performed by extracting the ligand, removing water molecules, adding hydrogen atoms and assigning AMBER7 FF99 charges to the protein. Compounds **8** and **14g** was docked into Akt1 and the hydrogen bonds and hydrophobic interactions were observed in the model, the best conformation with the highest CScore was selected for interaction analysis.

Acknowledgement

This work was supported by the Key Research and Development Project of Shandong Province (Nos. 2017CXGC1401 and 2019GSF108038)

Conflict of interest

The authors declare no conflict of interest.

References

[1] M. Martini, M.C. De Santis, L. Braccini, F. Gulluni, E. Hirsch, PI3K/AKT signaling pathway and cancer: an updated review, Annals of medicine 46(6) (2014) 372-83.
[2] P.S. Mundi, J. Sachdev, C. McCourt, K. Kalinsky, AKT in cancer: new molecular insights and advances in drug development, British journal of clinical pharmacology 82(4) (2016) 943-56.
[3] D. Massihnia, A. Avan, N. Funel, M. Maftouh, A. van Krieken, C. Granchi, R. Raktoe, U. Boggi, B. Aicher, F. Minutolo, A. Russo, L.G. Leon, G.J. Peters, E. Giovannetti, Phospho-Akt overexpression is prognostic and can be used to tailor the synergistic interaction of Akt inhibitors with gemcitabine in pancreatic cancer, Journal of hematology & oncology 10(1) (2017) 9.
[4] M.D. Ringel, N. Hayre, J. Saito, B. Saunier, F. Schuppert, H. Burch, V. Bernet, K.D. Burman, L.D. Kohn, M. Saji, Overexpression and overactivation of Akt in thyroid carcinoma, Cancer research 61(16) (2001) 6105-11.
[5] M. Cheung, J.R. Testa, Diverse mechanisms of AKT pathway activation in human malignancy, Current cancer drug targets 13(3) (2013) 234-44.
[6] A. Kumar, V. Rajendran, R. Sethumadhavan, R. Purohit, AKT Kinase Pathway: A Leading Target in Cancer Research %J The Scientific World Journal, 2013 (2013) 6.
[7] M. Song, A.M. Bode, Z. Dong, M.-H. Lee, AKT as a Therapeutic Target for Cancer, (2019).
[8] P. Jares, D. Colomer, E. Campo, Genetic and molecular pathogenesis of mantle cell lymphoma: perspectives for new targeted therapeutics, Nature reviews. Cancer 7(10) (2007) 750-62.
[9] P. Jares, D. Colomer, E. Campo, Molecular pathogenesis of mantle cell lymphoma, The Journal of clinical investigation 122(10) (2012) 3416-23.
[10] N. Vogt, B. Dai, T. Erdmann, W.E. Berdel, G. Lenz, The molecular pathogenesis of mantle cell lymphoma, Leukemia & lymphoma 58(7) (2017) 1530-1537.
[11] M. Rudelius, S. Pittaluga, S. Nishizuka, T.H. Pham, F. Fend, E.S. Jaffe, L. Quintanilla-Martinez, M. Raffeld, Constitutive activation of Akt contributes to the pathogenesis and survival of mantle cell lymphoma, Blood 108(5) (2006) 1668-76.
[12] Y. Oki, M. Fanale, J. Romaguera, L. Fayad, N. Fowler, A. Copeland, F. Samaniego, L.W. Kwak, S. Neelapu, M. Wang, L. Feng, A. Younes, Phase II study of an AKT inhibitor MK2206 in patients with relapsed or refractory lymphoma, British journal of haematology 171(4) (2015) 463-70.
[13] V.V. Prabhu, M.K. Talekar, A.R. Lulla, C.L.B. Kline, L. Zhou, J. Hall, A.P.J. Van den Heuvel, D.T. Dicker, J. Babar, S.A. Grupp, M.J. Garnett, U. McDermott, C.H. Benes, J.J. Pu, D.F. Claxton, N. Khan, W. Oster, J.E. Allen, W.S. El-Deiry, Single agent and synergistic combinatorial efficacy of first-in-class small molecule imipridone ONC201 in hematological malignancies, Cell cycle (Georgetown, Tex.) 17(4) (2018) 468-478.
[14] Y. Liu, Y. Yin, Z. Zhang, C.J. Li, H. Zhang, D. Zhang, C. Jiang, K. Nomie, L. Zhang, M.L. Wang, G. Zhao, Structural optimization elaborates novel potent Akt inhibitors with promising anticancer activity, European journal of medicinal chemistry 138 (2017) 543-551.
[15] Y. Liu, Y. Yin, J. Zhang, K. Nomie, L. Zhang, D. Yang, M.L. Wang, G. Zhao, Discovery of 4-(Piperazin-1-yl)-7H-pyrrolo[2,3-d]pyrimidine Derivatives as Akt Inhibitors, Archiv der Pharmazie 349(5) (2016) 356-62.
[16] D. Zhang, D. Tong, D. Yang, J. Sun, F. Zhang, G. Zhao, Design, synthesis and biological evaluation of AKT inhibitors bearing a piperidin-4-yl appendant, MedChemComm 9(8) (2018) 1340-1350.

[17] F. Chang, J.T. Lee, P.M. Navolanic, L.S. Steelman, J.G. Shelton, W.L. Blalock, R.A. Franklin, J.A. McCubrey, Involvement of PI3K/Akt pathway in cell cycle progression, apoptosis, and neoplastic transformation: a target for cancer chemotherapy, Leukemia 17(3) (2003) 590-603.
[18] S. Iyengar, A. Clear, C. Bodor, L. Maharaj, A. Lee, M. Calaminici, J. Matthews, S. Iqbal, R. Auer, J. Gribben, S. Joel, P110alpha-mediated constitutive PI3K signaling limits the efficacy of p110delta-selective inhibition in mantle cell lymphoma, particularly with multiple relapse, Blood 121(12) (2013) 2274-84.
[19] D.S. Levy, J.A. Kahana, R. Kumar, AKT inhibitor, GSK690693, induces growth inhibition and apoptosis in acute lymphoblastic leukemia cell lines, Blood 113(8) (2009) 1723-1729.
[20] E.K. Han, J. Leverson, T. McGonigal, O. Shah, K. Woods, T. Hunter, V. Giranda, Y. Luo, Akt inhibitor A-443654 induces rapid Akt Ser-473 phosphorylation independent of mTORC1 inhibition, Oncogene 26(38) (2007) 5655-5661.
[21] N. Rhodes, D.A. Heerding, D.R. Duckett, D.J. Eberwein, V.B. Knick, T.J. Lansing, R.T. McConnell, T.M. Gilmer, S.-Y. Zhang, K. Robell, Characterization of an Akt kinase inhibitor with potent pharmacodynamic and antitumor activity, Cancer research 68(7) (2008) 2366-2374.

Declaration of interests

☒ The authors declare that they have no known competing financial interests or personal relationships that could have appeared to influence the work reported in this paper.

☐The authors declare the following financial interests/personal relationships which may be considered as potential competing interests:

Continuous optimization of pyrrolopyrimidines as Akt inhibitors

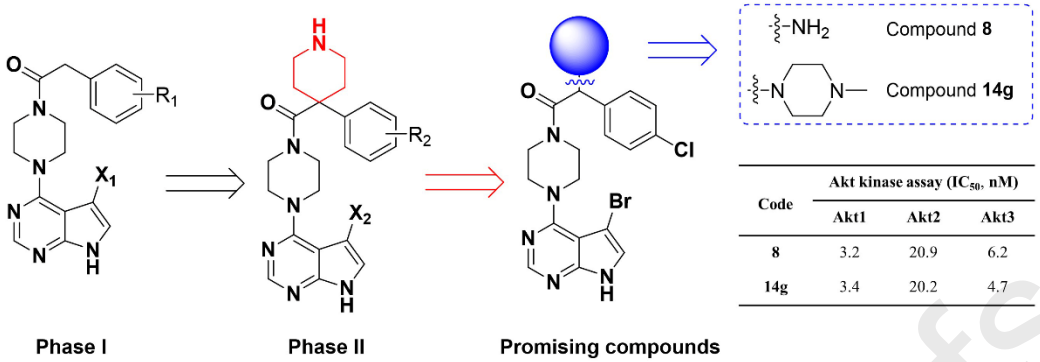

Code	Akt kinase assay (IC_{50}, nM)		
	Akt1	Akt2	Akt3
8	3.2	20.9	6.2
14g	3.4	20.2	4.7

Highlights

- Further exploration of pyrrolopyrimidine analogues as Akt inhibitors
- High enzymatic potency and antiproliferative effects in lymphoma cells
- Induction of cell apoptosis and G2/M cell cycle arrest
- Suppressed phosphorylation level of Akt downstream targets GSK3β and S6